

Extreme Image Compression using Fine-tuned VQGAN Models

Qi Mao, Tinghan Yang, Yinuo Zhang, Shuyin Pan, Meng Wang, Shiqi Wang, Siwei Ma

Abstract—Recent advances in generative compression methods have demonstrated remarkable progress in enhancing the perceptual quality of compressed data, especially in scenarios with low bitrates. Nevertheless, their efficacy and applicability in achieving extreme compression ratios (< 0.1 bpp) still remain constrained. In this work, we propose a simple yet effective coding framework by introducing vector quantization (VQ)-based generative models into the image compression domain. The main insight is that the codebook learned by the VQGAN model yields strong expressive capacity, facilitating efficient compression of continuous information in the latent space while maintaining reconstruction quality. Specifically, an image can be represented as VQ-indices by finding the nearest codeword, which can be encoded using lossless compression methods into bitstreams. We then propose clustering a pre-trained large-scale codebook into smaller codebooks using the K-means algorithm. This enables images to be represented as diverse ranges of VQ-indices maps, resulting in variable bitrates and different levels of reconstruction quality. Extensive qualitative and quantitative experiments on various datasets demonstrate that the proposed framework outperforms the state-of-the-art codecs in terms of perceptual quality-oriented metrics and human perception under extremely low bitrates.

Index Terms—Generative Compression, Extreme Compression, VQGANs, Low Bitrate.

I. INTRODUCTION

WITH the ever-increasing amount of visual data being generated at an unprecedented pace, the demand for highly efficient and effective compression algorithms has become increasingly crucial. However, under extremely limited network bandwidth, the signal-oriented traditional image/video compression codecs (e.g., BPG [1], and the latest video coding standard VVC [2]) inevitably adopt large scalar quantization steps, resulting in a significant loss of texture information with unacceptable blurring and blocking artifacts.

To bridge the gap of extremely low bitrate scenarios, recent image/video coding methods [3]–[15] leverage the power of generative models [16], [17] to reconstruct the human-favored decoded image/video. There are currently two main perspectives in such generative compression: the first [3],

[5], [7], [8] involves using a conditional GAN [18] as an additional distortion term to optimize deep learning-based end-to-end neural codecs. This category of methods enhances the reconstruction of texture details in the decoded image through adversarial training. However, their effectiveness in achieving high compression ratios, especially below 0.1 bpp, remains limited. Another line [4], [9]–[13] aims to compress images into compact feature representations at the encoding end and generate decoded images with the aid of GANs, achieving visual pleasing reconstruction even at extremely low compression ratios. However, without additional training, such approaches [9]–[12] have difficulty reconstructing the original image with large semantic information gaps against the training dataset. For instance, codecs optimized for face images may not perform well on natural scenario images. As such, their practical use in extremely low-bitrate scenarios is hindered by poor generalization ability.

Recently, vector quantization (VQ)-based generative models [21]–[25], which utilize discrete image representations, have been well-used in image generation tasks. Despite their success in other generation fields, VQ-based generative models have received relatively less attention in the image compression domain. In this work, we reveal a surprising finding: *The learned codebook of the VQGAN model [26], which has been trained on a large-scale dataset, exhibits a powerful and robust representational capacity.* On this basis, the integration of VQ-indices compression and fine-tuning the VQGAN model yields a significant advancement in the capability of extreme image compression, which exhibits generalizability across various semantics and resolutions of images.

Accordingly, we propose a novel coding framework that draws on the fundamental components of the VQGAN model. Specifically, we employ the VQGAN encoder to first transform images into their corresponding latent representations. Rather than compressing the latent features directly, our framework obtains VQ-indices by identifying the nearest sample in the learned codebook. These VQ-indices are then encoded into a bitstream using a lossless compression method. During the decoding process, the framework searches for the corresponding codewords based on their respective indices, generating the reconstructed latent representations. The VQGAN decoder then transforms these latent vectors back into the pixel space, ultimately resulting in the reconstruction of the decoded images. Furthermore, in the context of an unstable transmission environment, the loss of bitstreams can lead to the failure of the decoding process. To address this issue, we leverage the second-stage transformer of the VQGAN model to predict missing indices based on context indices

Qi Mao is with State Key Laboratory of Media Convergence and Communication, Communication University of China, Beijing 100024, China (e-mail: qimao@cuc.edu.cn) (corresponding author)

Tinghan Yang, Yinuo Zhang and Shuyin Pan are with School of Information and Communication Engineering, Communication University of China, Beijing 100024, China (e-mail: {yangtinghan, yinuozhang, psygkx}@cuc.edu.cn)

Meng Wang and Shiqi Wang are with the Department of Computer Science, City University of Hong Kong 999077, China (e-mail: mwang98-c@my.cityu.edu.hk, shiqi.wang@cityu.edu.hk)

Siwei Ma is with the National Engineering Research Center of Visual Technology, School of Computer Science, Peking University, Beijing 100871, China (e-mail: swma@pku.edu.cn)

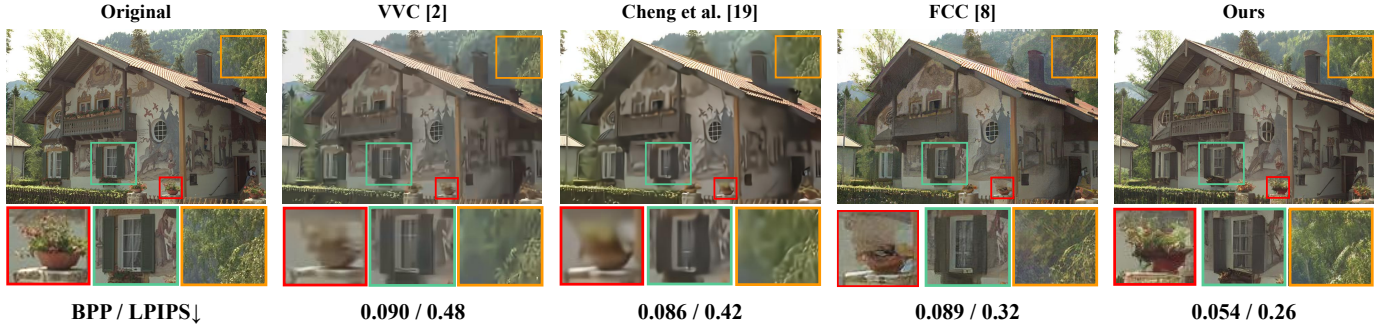


Fig. 1. Qualitative comparison results of the latest traditional video codec VVC [2], the pixel-optimization-oriented end-to-end neural codec Cheng *et al.* [19], the typical generative compression codec FCC [8], and our method on the Kodak dataset [20]. The bpp and LPIPS metrics of each method are provided at the bottom, with a lower value indicating better performance. Our method outperforms the other codecs with the best perceptual quality at the lowest bitrates.

that adhere to the underlying discrete distribution, thereby effectively circumventing image reconstruction failure due to the loss of bitstreams.

VQ-indices play a pivotal role in the proposed image compression framework. The learned codebook’s remarkable expressive capacity allows for the compression of continuous information in the latent space while ensuring high-quality reconstruction. Consequently, the codebook’s size, a crucial factor determining its representational capacity, has a profound influence on both compression ratio and reconstruction quality. To enable variable bitrates, we propose clustering a pre-trained large-scale codebook using the K-means algorithm, resulting in a series of smaller codebooks. The entire model is then fine-tuned based on this modified framework. As a consequence, the image can be represented by various VQ-indices maps, resulting in variable bitrates and different levels of reconstruction quality.

We evaluate the proposed framework on a wide range of image datasets. Both qualitative and quantitative results demonstrate that the proposed framework achieves significant improvement against the state-of-the-art codecs in terms of both perceptual quality metrics and human-viewed, as demonstrated in Fig. 1. Moreover, in cooperation with the second-stage generative transformer model, missing indices can be restored well when the loss ratio is not high ($\leq 20\%$). Overall, the proposed image codecs based on the VQGAN model can overcome the limitations of existing codecs in achieving high perceptual quality at extremely low bitrates, offering a promising direction for research in the field of ultra-low bitrate compression. The main contributions in this paper can be summarized as follows:

- We present one of the pioneering efforts to utilize the VQGAN model in developing a novel image compression framework that aims to achieve high perceptual quality reconstruction at significantly low bitrates.
- We develop a second-stage transformer to predict the missing indices, enhancing the resilience of the proposed framework in unstable transmission.
- We propose a K-means clustering approach to compress the large-scale codebook and derive a smaller new codebook, which enables variable bitrates and varying levels of reconstruction quality within our framework.

II. RELATED WORKS

A. Generative Compression

For several decades, classical image and video coding technologies [2], [27]–[31] have been widely used. With the continuous development of large-scale data-driven deep models, image compression methods based on deep neural networks (DNN) have shown promising results compared to classical codecs. Recent research efforts have focused on designing more flexible variable bitrate strategies [32]–[35], constructing better transformations from image space to latent space [36]–[39], and developing more accurate entropy estimation models [19], [40]–[47]. However, these methods tend to produce blurry reconstructions in low-bitrate scenarios due to optimization only targeting pixel-level objectives.

In recent years, there have been two main approaches proposed by generative compression methods to achieve high-quality compression at low bitrates. The first line of approaches uses conditional adversarial loss as a distortion loss term to guide end-to-end optimization [3], [5]–[8]. These methods have shown significant improvements in the subjective perceptual quality of image reconstruction. Nevertheless, they still face challenges in achieving satisfactory performance under ultra-low bitrates ($< 0.1\text{bpp}$). The other line of approaches [4], [9]–[13] compresses images into compact feature representations at the encoder end and uses generative models to generate high-quality images at the decoder end. For example, Chang *et al.* [9]–[12] encode images into structural features and low-dimensional texture features as compact representations, facilitating the extremely low compression ratios. However, the above methods are limited in generalizability and cannot generate the expected texture in scenarios with a significant semantic gap between the training and testing domains. Moreover, separate models must be trained to cope with different resolution sizes for optimal performance. Therefore, such limitations restrict their practical application scenarios.

In this work, we propose a coding framework that effectively combines the principles of generative compression with the VQGAN model. Instead of employing latent representations to encode images, our framework utilizes a learned codebook serving as the nearest neighbor lookup to quantize

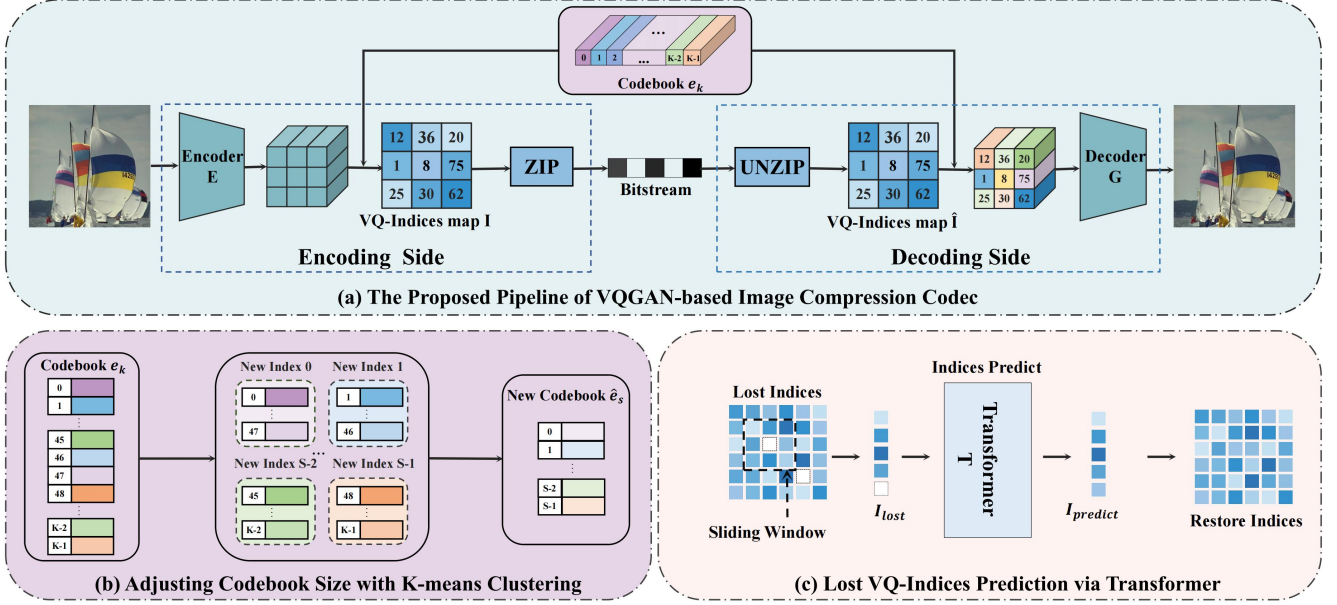


Fig. 2. **Overview of the proposed VQGAN-based image coding framework.** (a) the overall compression pipeline; (b) the K-means clustering algorithm to adjust the codebook size for variable bitrates; (c) lost VQ-indices prediction via the transformer.

the latent embedding into discrete VQ-indices, resulting in significant compression of the corresponding information. By virtue of the high representational capacity of the VQGAN model’s codebook, our framework overcomes the generalization shortcoming and surpasses the performance of the latest codecs in extremely low-bitrate scenarios.

B. VQ-based Generative Models

The advent of VQVAE [48], which employs discrete image representations, has recently sparked considerable interest in VQ-based generative models. Generally, VQ-based generative models comprise two stages. In the first stage, an encoder-decoder quantizer is trained to obtain the latent variables of an image and quantize them using the learned codebook. In the second stage, a prior network is employed to model the distribution in the discrete space. VQGAN [26] has enhanced the quality of generated images by incorporating adversarial learning [16] and perceptual loss [49] into the VQVAE [48]. Moreover, VQGAN replaces pixel-CNN [50] with a transformer [51] model as the prior model, allowing for the generation of high-resolution images. There has been subsequent research aimed at improving the generation quality of VQ-based models by focusing on enhancing the reconstruction fidelity [22], [52], [53]. Additionally, the second stage has been enhanced by the introduction of a bi-directional non-autoregressive transformer [23], [24]. VQ-based generative models have been applied in various generative tasks, including image generation [21]–[23], video generation [54]–[56], text-to-image generation [57], [58], and face restoration [59], [60]. Despite the growing success in image synthesis, their application to image compression has received relatively less attention. This work aims to bridge this gap by demonstrating

how the VQGAN model can be utilized to power image compression under extremely low compression.

III. PROPOSED VQGAN-BASED EXTREME IMAGE CODEC

In this work, we aim to compress images at ultra-low bit rates while maintaining the high-perceived quality of the reconstructed images. Our framework is built upon the discrete representations and generative capacity of VQGAN models. As illustrated in Fig. 2, the proposed pipeline consists of four key components:

- The encoder E : extract the input image $\mathbf{x} \in \mathbb{R}^{H \times W \times 3}$ into a latent representation $\mathbf{z} \in \mathbb{R}^{\frac{H}{M} \times \frac{W}{M} \times n_z}$.
- The codebook $\mathbf{e}_k \in \mathbb{R}^{n_z}, k \in 1, 2, \dots, K$: map the latent representation \mathbf{z} into a sequence of VQ-indices and invert it back to quantized latent representation $\mathbf{z}_q \in \mathbb{R}^{\frac{H}{M} \times \frac{W}{M} \times n_z}$ through the nearest neighbor lookup. The proposed K-means clustering algorithm method compresses the large-scale codebook into a smaller one, enabling variable bitrates and varying reconstruction quality.
- The decoder G : synthesize the quantized latent representation \mathbf{z}_q into reconstructed image $\hat{\mathbf{x}} \in \mathbb{R}^{H \times W \times 3}$.
- The transformer T : predict the missing index on the basis of the context indices.

On the encoding side, VQ-indices are compressed into the final bitstream using lossless compression techniques, *i.e.*, ZIP [61], [62]. On the decoding side, we decode the index sequences from the bitstream and convert the decoded VQ-indices back into the quantized latent representation \mathbf{z}_q by searching the codeword from the codebook. In the following, we detail the compression methodologies (Section III-A), the training strategies (Section III-B), and the lost index prediction approach (Section III-C) of the proposed framework.

A. VQ-indices Compression

VQ is a classic quantization technique used in data compression to reduce the size by representing a set of similar data points with a single representative vector, which efficiently represents the data while preserving its essential features. Unlike existing neural image compression methods [19], [32]–[35] that adopt scalar-quantization, we leverage the power of VQ to construct a codebook of representative vectors for latent representations \mathbf{z} . In particular, the codebook \mathbf{e}_k is then used to encode the latent representation by replacing each position of a vector with the **index** of the closest representative vector by Euclidean distance, which results in a highly compressed version of the latent representation with a minimal loss of quality:

$$\mathbf{I}_{ij} = \underset{k \in \{1, 2, \dots, K\}}{\operatorname{argmin}} \|\mathbf{z}_{ij} - \mathbf{e}_k\|^2, \quad (1)$$

where i and j denote the position of vector \mathbf{z}_{ij} in latent representation \mathbf{z} , \mathbf{I}_{ij} represents its corresponding index, and K indicates the size of codebook.

Accordingly, an input image \mathbf{x} can be efficiently represented by VQ-indices map $\mathbf{I} \in \mathbb{R}^{\frac{H}{M} \times \frac{W}{M}}$, which significantly reduces the data amount. Then, we adopt the widely used lossless compression method ZIP [61], [62] to compress VQ-indices into bitstreams, further reducing the data size. After decoding the compressed bitstream, the reconstructed latent vectors \mathbf{z}_q are generated by searching for their corresponding code words based on their indices. Finally, the reconstructed image $\hat{\mathbf{x}}$ is synthesized by the decoder G .

Adjusting Variable Bitrates. The quality of the codebook in our proposed framework plays a crucial role in determining the compression performance of the entire system. As such, we develop a rate control strategy that enables the flexible adjustment of compression bitrates by altering the size of the codebook. In particular, we propose to utilize the K-means algorithm to cluster large-scale codebooks, allowing us to obtain centroids for each cluster. After modifying its size, these centroids are used as initial values for each codebook vector. By doing so, we are able to obtain new codebooks of varying sizes, each with a corresponding set of VQ-indices to represent the compressed image. On this basis, we are capable of employing flexible codebook resizing while ensuring codebook quality.

In detail, the initialization of K-means clustering algorithm first randomly assigns centroids of the already trained large-scale codebook \mathbf{e}_k . Then, the Euclidean distance between each codebook vector and each centroid is computed to assign the vector to the closest centroid as:

$$C_s = \underset{s \in \{1, 2, \dots, S\}}{\operatorname{argmin}} \|\mathbf{e}_k - \hat{\mathbf{e}}_s\|^2, \quad (2)$$

where C_s is the s -th cluster, $\hat{\mathbf{e}}_s$ denotes its cluster centroids, and $S (S < K)$ is the new size of the codebook. Subsequently, for each cluster, the mean of the codebook vectors within the cluster C_j is recalculated, and the cluster centroids are updated accordingly:

$$\hat{\mathbf{e}}_s = \frac{1}{|C_s|} \sum_{\mathbf{e} \in C_s} \mathbf{e}. \quad (3)$$

The above-mentioned steps are iteratively performed until the resulting clustering outcome minimizes the associated cost function:

$$\min J(\mathbf{e}_k; \hat{\mathbf{e}}_s) = \min \left(\frac{1}{K} \sum_{k=1}^K \|\mathbf{e}_k - \hat{\mathbf{e}}_s\|^2 \right). \quad (4)$$

As a consequence, the newly generated codebook $\hat{\mathbf{e}}_s$ derived from the above K-means clustering algorithm can serve as a starting point for further fine-tuning, enabling faster convergence during subsequent optimization.

B. Training Strategies

Our proposed framework aims to minimize the distortion between the reconstructed image $\hat{\mathbf{x}}$ and the original image \mathbf{x} . Given that a codebook plays a vital role for VQ in the encoding process, it is crucial to ensure the quality of the codebook during training. As such, the loss for the generator should be designed as follows:

$$\mathcal{L}_{VQ}(E, G, \hat{\mathbf{e}}_s) = \|\mathbf{x} - \hat{\mathbf{x}}\|^2 + \|sg[E(\mathbf{x})] - \mathbf{z}_q\|_2^2 + \|sg[\mathbf{z}_q] - E(\mathbf{x})\|_2^2, \quad (5)$$

Here, $sg[\cdot]$ denotes the stop-gradient operation. To enhance the richness of the learned codebooks and improve the image perceptual quality, we incorporate adversarial loss and perceptual loss into our approach, as [26]. Specifically, we replace the L_2 loss in Eq.(5) with perceptual loss [49] and introduce a patch-based discriminator (D) [65] using an adversarial training procedure to differentiate between real and decoded images,

$$\mathcal{L}_{GAN}(\{E, G, \hat{\mathbf{e}}_s\}, D) = [\log D(\mathbf{x}) + \log(1 - D(\hat{\mathbf{x}))]. \quad (6)$$

Therefore, the objective for finding the optimal compression model $\mathcal{Q}^* = \{E^*, G^*, \hat{\mathbf{e}}_s^*\}$ as:

$$\mathcal{Q}^* = \underset{E, G, \hat{\mathbf{e}}_s}{\operatorname{argmin}} \max_D \mathbb{E}_{\mathbf{x} \sim p(\mathbf{x})} \left[\mathcal{L}_{VQ}(E, G, \hat{\mathbf{e}}_s) + \lambda \mathcal{L}_{GAN}(\{E, G, \hat{\mathbf{e}}_s\}, D) \right], \quad (7)$$

here, λ is calculated by the following formula as,

$$\lambda = \frac{\nabla_{GL}[\mathcal{L}_{rec}]}{\nabla_{GL}[\mathcal{L}_{GAN}] + \delta}, \quad (8)$$

where \mathcal{L}_{rec} represents the perceptual loss, $\nabla_{GL}[\cdot]$ denotes the gradient of the last layer L of the decoder, and $\delta = 10^{-6}$ is used to maintain numerical stability.

C. Lost VQ-indices Prediction

In an unreliable transmission environment, lost packets may result in the loss of indices, which can cause incorrect decoding of bitstreams. However, our proposed image codec framework, which utilizes the transformer, can accurately predict lost indices at the decoder end. This approach enhances the robustness of the codec in dealing with unreliable network transmission and ensures that the decoded bitstreams remain accurate.

As illustrated in Section III-A, an image \mathbf{x} can be efficiently represented by VQ-indices map \mathbf{I} . We flatten the VQ-indices



Fig. 3. The qualitative comparison results of BPG [1], VVC [2], Cheng *et al.* [19], ours w/o fine-tune and our method on the Kodak dataset [20]. The bpp and LPIPS of each method are shown at the bottom of each image. In particular, ↓ indicates that lower is better.

map, and denote it as $[\mathbf{I}_i]_{i=1}^N$, where N indicates the total length. Subsequently, the VQGAN's second-stage transformer is trained to predict the probability distribution of the next possible indices $p(\mathbf{I}_i | \mathbf{I}_{<i})$. The objective is to maximize the log-likelihood of the data representation, which can be expressed as follows:

$$\mathcal{L}_T = \mathbb{E}_{\mathbf{x} \sim p(\mathbf{x})} [-\log p(\mathbf{I})], \quad (9)$$

where $p(\mathbf{I}) = \prod_i p(\mathbf{I}_i | \mathbf{I}_{<i})$. To simulate the potential loss of indices during transmission, we incorporate a **masking** procedure. Specifically, we apply a binary mask $M = [m_i]_{i=1}^N$ as follows: For $m_i = 1$, the corresponding index \mathbf{I}_i is replaced by a special $[mask]$ token to indicate that it has been lost. Conversely, if $m_i = 0$, then \mathbf{I}_i is left unchanged. The mask process is controlled by a mask ratio ($\alpha \in [0, 1]$), which determines the number of missing indices as $\alpha \cdot N$, denoted as \mathbf{I}_{lost} . During the storage stage, as depicted in Fig. 2(c), it is possible to predict the probabilities of all potential indices in the codebook for each lost position i . However, due to the

attention mechanism of the transformer that limits the length N of its input sequence, a sliding window input strategy is employed to input a 16×16 window centered on \mathbf{I}_i at each prediction. Only the indices before i in the 16×16 window are included as input due to the autoregressive nature of the transformer, which is consistent with the decoding process. This approach better utilizes the spatial structure of the image. The predicted index $\hat{\mathbf{I}}_i$ is obtained upon sampling. Subsequently, the restored image $\hat{\mathbf{x}}$ is generated by feeding the predicted index sequence $\mathbf{I}_{predict}$ into the decoder G .

IV. EXPERIMENTS

A. Experimental Settings

DataSets. The proposed framework is trained on the ImageNet dataset [66], which contains 1.2 million images distributed across 1,000 distinct categories. To assess the performance of the proposed model, we conduct an evaluation on three commonly used datasets in image compression: the Kodak dataset

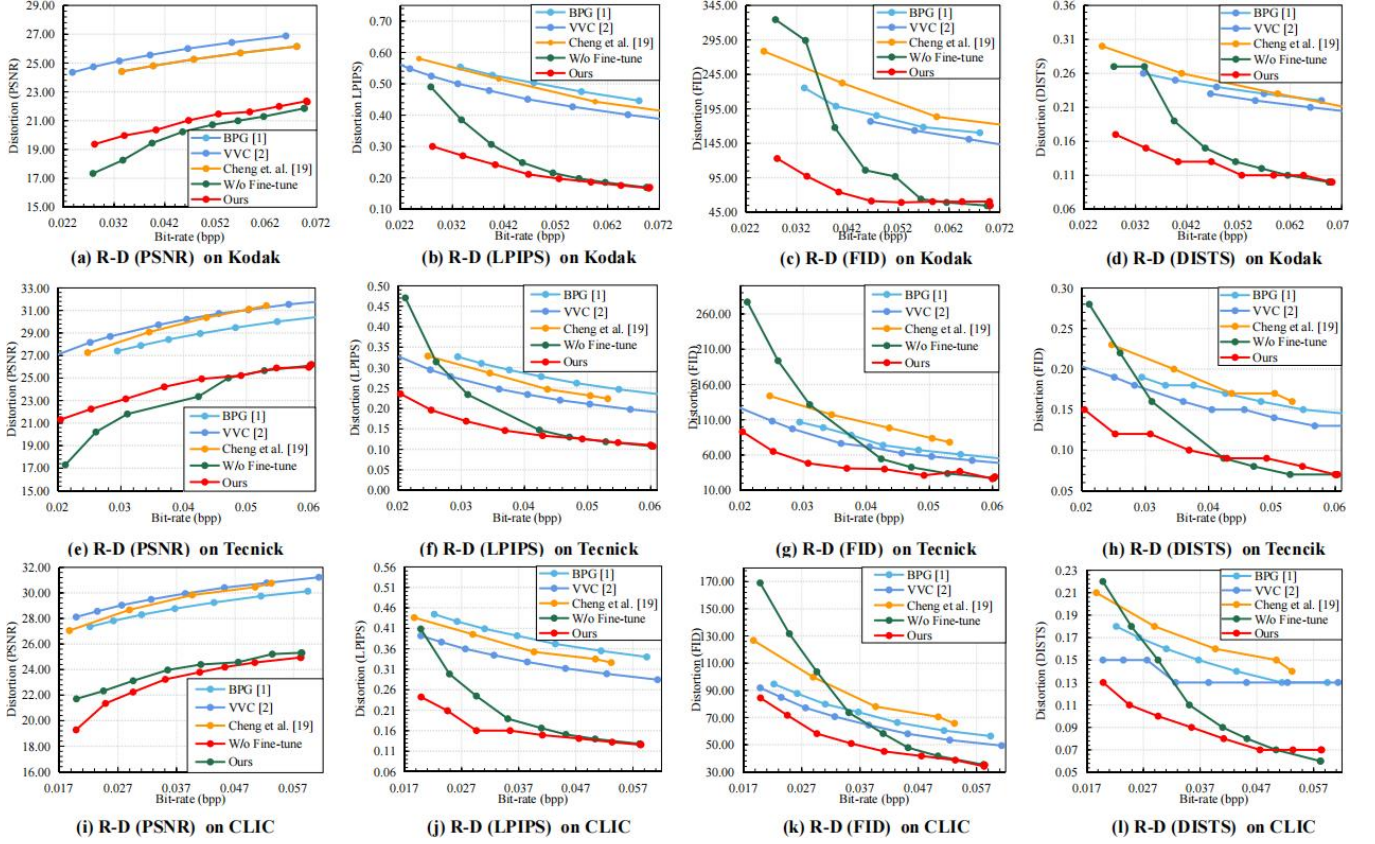


Fig. 4. The R-D performance of BPG [1], VVC [2], Cheng *et al.* [19], ours w/o fine-tune and our method on the Kodak dataset [20], the CLIC2020 dataset [63], and the Tecnick dataset [64]. (a), (e), and (i) Higher PSNR value indicates higher signal fidelity; (b), (c), (d), (f), (g), (h), (j), (k), and (l) Lower LPIPS, FID, and DISTS values indicate better perceptual quality.

[20], which includes 24 natural uncompressed 512×768 or 768×512 images; the CLIC2020 dataset [63], comprising 250 images that exhibit varying lighting conditions and dynamic range, with resolutions ranging from 320×240 to 4032×3024 ; and the Tecnick dataset [64], which consists of 40 images in resolution of 1200×1200 .

Implementation Details. Our proposed approach is implemented using PyTorch Lightning and trained on two NVIDIA Tesla-A100 GPUs. We adopt $M = 16$ to downsample the image \mathbf{x} into the latent representation \mathbf{z} . First, the weights of encoder E , decoder G , and the discriminator D are initialized by the officially provided pre-trained VQ-GAN model¹. To enable the proper bitrate range, we perform Kmeans clustering on the size of 16384 codebook of the pre-trained model, reducing the new codebooks into the size, ranging from $\{2048, 1024, 512, 256, 128, 64, 32, 16, 8\}$. We then fine-tune the entire framework using the default settings as [26].

Evaluation Metrics. We start by employing the commonly used signal-oriented metric Peak Signal-to-Noise Ratio (PSNR). Then, we integrate recent approaches to assess perceptual quality, which better aligns with the way humans perceive images. In particular, the learned perceptual image patch similarity (LPIPS) [67] and the deep image structure and texture similarity (DISTS) [68] metrics are adopted. LPIPS calculates distance within the feature space of the AlexNet

embedding, while DISTS unifies structure and texture similarity using deep features to more accurately capture texture perception. Additionally, we employ the Frechet Inception Distance (FID) [69], a widely used metric for evaluating image quality in image generation tasks. FID measures the similarity between the distribution of the distorted images and the distribution of the reference images. Furthermore, we utilize bits per pixel (bpp) to evaluate the rate performance.

B. Compression Performance Comparison

Compared Methods. To evaluate the efficacy of our proposed framework, we compare the proposed method with both traditional standard and neural-based typical compression frameworks: First, we compare with classic image codec BPG and the latest video coding codec VVC [2]. We utilize BPG [1] to encompass the bitrate range of our proposed method with QP values ranging from $\{51, 50, 49, 48, 47, 46, 45, 44\}$. We employ all intra configuration of the reference software VTM-11.0² and use QP = $\{51, 50, 49, 48, 47\}$ to cover the bitrate range of our proposed method. For typical deep learning-based end-to-end (E2E) codec, we compare with Cheng *et al.* [19] and retrain the model implemented by CompressAI³ to cover the similar bitrate range as ours. Specifically, we adopt the $\lambda = \{27, 45, 75, 100, 110\} \times 10^{-5}$. Furthermore, we develop

¹<https://github.com/CompVis/taming-transformers>

²https://vcgit.hhi.fraunhofer.de/jvet/VVCSSoftware_VTM/-/tree/master

³<https://github.com/InterDigitalInc/CompressAI>

TABLE I
BD-RATE AND BD-METRIC RELATIVE TO THE BPG [1], VVC [2], CHENG *et al.* [19] AND OURS W/O FINE-TUNE RESPECTIVELY, WHERE LPIPS IS USED AS THE DISTORTION METRIC IN BD-METRIC.

Baselines	Kodak [20]		CLIC2020 [63]		Techick [64]	
	BD-rate	BD-LPIPS	BD-rate	BD-LPIPS	BD-rate	BD-LPIPS
BPG [1]	-91.45%	-0.25	-96.74%	-0.23	-66.31%	-0.14
VVC [2]	-80.93%	-0.23	-78.58%	-0.17	-52.04%	-0.09
Cheng <i>et al.</i> [19]	-89.87%	-0.27	-96.28%	-0.21	-57.08%	-0.13
Ours w/o Fine-tune	-14.94%	-0.06	-20.09%	-0.05	-18.52%	-0.06

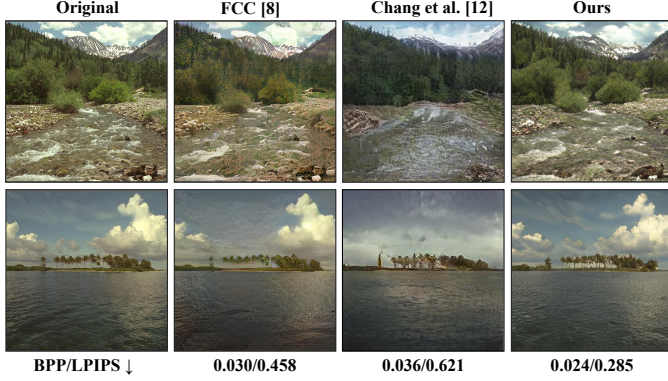


Fig. 5. Qualitative comparisons of two typical generative compression codecs (*i.e.*, FCC [8], Chang *et al.* [12]) and the proposed method over the Kodak dataset [20]. The average bpp and LPIPS of each the method is reported at the bottom row.

an additional variant that directly adopt the K-means clustering algorithm without any fine-tuning, denoted as "Ours w/o fine-tune".

Qualitative Evaluation. Fig. 3 shows the reconstruction results of various methods on different images on the Kodak dataset [20], as well as the corresponding bpp and LPIPS. In particular, we present a range of bitrates, specifically ranging from 0.04 to 0.1 bpp of reconstructed images, facilitating a comprehensive evaluation of the methods. It is evident that at extremely low bitrates, VVC [2], BPG [1], and Cheng *et al.* [19] exhibit varying degrees of blurring and missing texture details. In contrast, our proposed method reconstructs more texture details, such as trees, ripples, clouds, and feathers, resulting in the lowest LPIPS value. Hence, our proposed scheme can offer more accurate detail reconstruction, aligning with human visual requirements and exhibiting better compression performance at lower bitrates. Moreover, it is noteworthy that models obtained using the K-means clustering algorithm can produce relatively rich details even without fine-tuning training, thanks to the inherent expressive power of the pre-trained codebook. Nevertheless, upon fine-tuning, our proposed method outperforms the former by achieving more color and texture reconstruction consistency. This observation highlights the effectiveness of fine-tuning in enhancing model performance.

Quantitative Evaluation. Regarding quantitative evaluations, we show the rate-distortion (R-D) performance over different methods on the three datasets, as illustrated in Fig. 4. The experimental results demonstrate the effectiveness of our proposed bit rate control strategy, as evidenced by the decreasing compression bit rate as the size of the K-means clustering codebook decreases. Similar to other generative compression

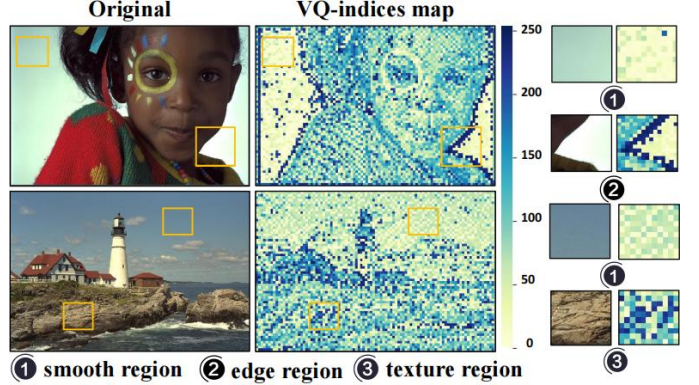


Fig. 6. **VQ-indices map visualization.** In the heat map, the larger the index, the darker the annotation color. The selected image patches within the boxes correspond to specific regions labeled according to their respective numbers.

methods, the performance of our model is not significant in terms of the signal-oriented PSNR metric. Nevertheless, our proposed approach exhibits remarkable improvements in perceptual-oriented metrics compared to other compression methods. To better evaluate the RD performance improvement of our proposed method, we utilize the Bjontegaard metric [70], as demonstrated in Table III. For instance, with the same reconstruction quality of the LPIPS metric, our approach achieves approximately 66.31% ~ 96.74%, 52.04% ~ 80.93%, 57.08% ~ 96.28% bitrates saving compared to VVC, BPG, and Cheng *et al.* [19] over the three datasets, respectively. These results demonstrate the remarkable advantage of our proposed method achieving high perceptual quality for extremely low bitrate coding. The performance of models generated by utilizing the K-means clustering algorithm without fine-tuning can yield promising results on the rate-distortion (R-D) curve when the size of the codebook is relatively large. Nonetheless, a significant degradation in performance is observed when the size of the codebook is reduced to below 64. Fine-tuning can effectively enhance the performance of the model under such conditions, with 14.94% ~ 20.09% bitrates saving, as shown in Table III.

C. Comparisons with Generative Image Compression Codecs.

To comprehensively assess the efficacy and applicability of the proposed approach vis-a-vis state-of-the-art generative compression codecs, we perform comparative analyses against two representative codecs using their officially provided models, as illustrated in Fig. 5. FCC [8] is among the first line of approaches that utilize adversarial loss to optimize the end-to-end framework, capable of achieving extremely low bitrates below 0.1 bpp. Nevertheless, it exhibits suboptimal

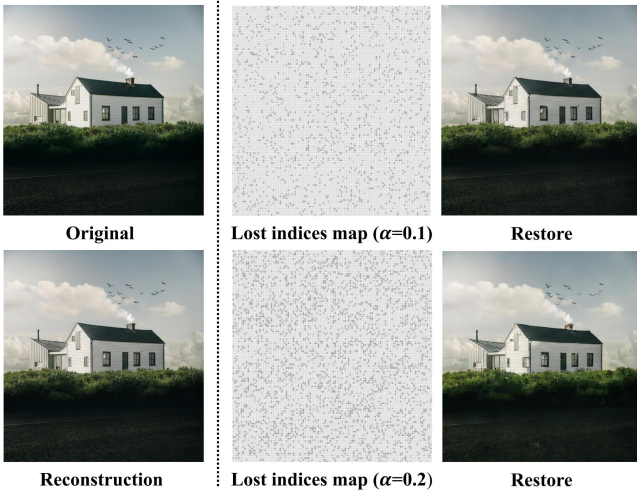


Fig. 7. **Image restoration via lost VQ-indices prediction under $\alpha = 0.1, 0.2$.** Additionally, we provide a visualization of the lost indices map, where in darker colors denote lost indices. Furthermore, we present a visual graph of the lost indices map, in which the black color corresponds to the indices that have been lost.

performance in the presence of artifacts resembling colored dots. Chang *et al.* [12] encodes images into semantic maps and corresponding texture features. We compare our method with the model trained on the ADE20K outdoor dataset. Despite achieving high compression ratios, Chang *et al.* [12]’s method suffers from poor generalization ability in the presence of a semantic gap between the training and testing domains, resulting in inadequate texture generation. Compared to the original image, notable differences in both chromaticity and texture are evident. For instance, the reconstructed image fails to capture the clouds present in the original image, leading to the worst LPIPS value. In contrast, our method exhibits superior performance and generalization in generating reconstructed images with both subjective perception and objective metrics, even at extremely low bitrates (0.024 bpp).

D. Analysis and Discussions

Visualization of VQ-indices Map. To facilitate a better understanding of the relationship between the image semantic content and the codebook, we reorder the VQ-indices in direct proportion to the L_2 distances among codebook vectors, as shown in Fig. 6. The codewords can effectively reflect the distribution of semantic content in the image. Smooth regions of an image typically select VQ-indices that are either identical or have small distances between them, while more complex regions such as those containing texture or edges tend to employ VQ-indices that are significantly different in distance. This can result in more intricate color variations and distinct structural boundaries.

Lost VQ-indices Prediction. Fig. 7 presents a visualization of the lost indices map at 10% and 20% loss ratios, as well as the corresponding restored images, generated via the utilization of indices predicted by the transformer model. Evidently, the restored images display a similar degree of fidelity to the reconstructed image without indices missing, thereby suggesting that the indices can be accurately predicted

TABLE II
ABLATION STUDIES ON THE EFFECTIVENESS OF K-MEANS CLUSTERING ON THE KODAK DATASET [20]. LOWER BPP AND LPIPS INDICATE BETTER PERFORMANCE. BOLD INDICATES THE BEST SCORE.

Methods	bpp ↓	LPIPS ↓
Random initialization	0.026	0.33
Ours	0.070	0.17

when the levels of missing data are not particularly significant (*i.e.*, less than 20%).

Effectiveness of K-means Clustering. To evaluate the significance of using K-means clustering as the starting point for the fine-tuning process, we conduct an ablation study by initializing the codebook randomly instead of employing K-means clustering. The results are presented in Table IV, where we observe that although the method using a randomly initialized codebook achieves a large bitrate reduction, the reconstructed quality is significantly inferior. This finding indicates that the pre-trained codebook’s expressive power can be considered a robust prior, which significantly contributes to preserving the quality of reconstruction.

V. CONCLUSIONS

In this work, we propose a novel scheme that utilizes the VQ-indices maps obtained from VQGANs as compact visual data representations to achieve extremely high image compression ratios while maintaining perceptual quality. Our proposed scheme uniquely adjusts the quantization step by varying the size of codebooks through the K-means clustering and recovers missing indices by the transformer, enabling reliable compression with variable bit rates and varying levels of reconstruction quality. Qualitative and quantitative results demonstrate the superiority of our proposed scheme in perceptual quality at extremely low bit rates compared to state-of-the-art codecs. Furthermore, our method addresses the limitations of resolution and dataset in extreme image compression and shows superiority in generalization and reliable transmission, as evidenced by experiments on various datasets. Overall, our work advances image/video coding research by demonstrating the potential of VQ-based generative models for research in ultra-low bitrate compression.

REFERENCES

- [1] Fabrice Bellard, “Bpg image format,” <https://bellard.org/bpg/>, 2018.
- [2] Benjamin Bross, Ye-Kui Wang, Yan Ye, Shan Liu, Jianle Chen, Gary J Sullivan, and Jens-Rainer Ohm, “Overview of the versatile video coding (vvc) standard and its applications,” *IEEE Transactions on Circuits and Systems for Video Technology*, vol. 31, no. 10, pp. 3736–3764, 2021.
- [3] Oren Rippel and Lubomir Bourdev, “Real-time adaptive image compression,” in *International Conference on Machine Learning*. PMLR, 2017, pp. 2922–2930.
- [4] Shibani Santurkar, David Budden, and Nir Shavit, “Generative compression,” in *2018 Picture Coding Symposium (PCS)*. IEEE, 2018, pp. 258–262.
- [5] Eirikur Agustsson, Michael Tschannen, Fabian Mentzer, Radu Timofte, and Luc Van Gool, “Generative adversarial networks for extreme learned image compression,” in *Proceedings of the IEEE/CVF International Conference on Computer Vision*, 2019, pp. 221–231.
- [6] Jooyoung Lee, Donghyun Kim, Younhee Kim, Hyoungjin Kwon, Jongho Kim, and Taejin Lee, “A training method for image compression networks to improve perceptual quality of reconstructions,” in *Proceedings of the IEEE/CVF Conference on Computer Vision and Pattern Recognition Workshops*, 2020, pp. 144–145.

- [7] Fabian Mentzer, George D Toderici, Michael Tschannen, and Eirikur Agustsson, "High-fidelity generative image compression," *Advances in Neural Information Processing Systems*, vol. 33, pp. 11913–11924, 2020.
- [8] Shoma Iwai, Tomo Miyazaki, Yoshihiro Sugaya, and Shinichiro Omachi, "Fidelity-controllable extreme image compression with generative adversarial networks," in *2020 25th International Conference on Pattern Recognition (ICPR)*, IEEE, 2021, pp. 8235–8242.
- [9] Jianhui Chang, Qi Mao, Zhenghui Zhao, Shanshe Wang, Shiqi Wang, Hong Zhu, and Siwei Ma, "Layered conceptual image compression via deep semantic synthesis," in *2019 IEEE International Conference on Image Processing (ICIP)*, IEEE, 2019, pp. 694–698.
- [10] Jianhui Chang, Zhenghui Zhao, Lingbo Yang, Chuanmin Jia, Jian Zhang, and Siwei Ma, "Thousand to one: Semantic prior modeling for conceptual coding," in *2021 IEEE International Conference on Multimedia and Expo (ICME)*, IEEE, 2021, pp. 1–6.
- [11] Jianhui Chang, Zhenghui Zhao, Chuanmin Jia, Shiqi Wang, Lingbo Yang, Qi Mao, Jian Zhang, and Siwei Ma, "Conceptual compression via deep structure and texture synthesis," *IEEE Transactions on Image Processing*, vol. 31, pp. 2809–2823, 2022.
- [12] Jianhui Chang, Jian Zhang, Youmin Xu, Jiguo Li, Siwei Ma, and Wen Gao, "Consistency-contrast learning for conceptual coding," in *Proceedings of the 30th ACM International Conference on Multimedia*, 2022, pp. 2681–2690.
- [13] Fei Yang, Yaxing Wang, Luis Herranz, Yongmei Cheng, and Mikhail G Mozerov, "A novel framework for image-to-image translation and image compression," *Neurocomputing*, vol. 508, pp. 58–70, 2022.
- [14] Mustafa Shukor, Bharath Bhushan Damodaran, Xu Yao, and Pierre Hellier, "Video coding using learned latent gan compression," in *Proceedings of the 30th ACM International Conference on Multimedia*, 2022, pp. 2239–2248.
- [15] Ruofan Wang, Qi Mao, Shiqi Wang, Chuanmin Jia, Ronggang Wang, and Siwei Ma, "Disentangled visual representations for extreme human body video compression," in *2022 IEEE International Conference on Multimedia and Expo (ICME)*, IEEE, 2022, pp. 1–6.
- [16] Ian Goodfellow, Jean Pouget-Abadie, Mehdi Mirza, Bing Xu, David Warde-Farley, Sherjil Ozair, Aaron Courville, and Yoshua Bengio, "Generative adversarial networks," *Communications of the ACM*, vol. 63, no. 11, pp. 139–144, 2020.
- [17] Diederik P Kingma and Max Welling, "Auto-encoding variational bayes," *arXiv preprint arXiv:1312.6114*, 2013.
- [18] Mehdi Mirza and Simon Osindero, "Conditional generative adversarial nets," *arXiv preprint arXiv:1411.1784*, 2014.
- [19] Zhengxue Cheng, Heming Sun, Masaru Takeuchi, and Jiro Katto, "Learned image compression with discretized gaussian mixture likelihoods and attention modules," in *Proceedings of the IEEE/CVF Conference on Computer Vision and Pattern Recognition*, 2020, pp. 7939–7948.
- [20] Eastman Kodak, "Kodak photocd dataset," <http://r0k.us/graphics/kodak/>, 2013.
- [21] Yuchao Gu, Xintao Wang, Yixiao Ge, Ying Shan, Xiaohu Qie, and Mike Zheng Shou, "Rethinking the objectives of vector-quantized tokenizers for image synthesis," *arXiv preprint arXiv:2212.03185*, 2022.
- [22] Jiahui Yu, Xin Li, Jing Yu Koh, Han Zhang, Ruoming Pang, James Qin, Alexander Ku, Yuanzhong Xu, Jason Baldridge, and Yonghui Wu, "Vector-quantized image modeling with improved vqgan," *arXiv preprint arXiv:2110.04627*, 2021.
- [23] Huiwen Chang, Han Zhang, Lu Jiang, Ce Liu, and William T Freeman, "Maskgit: Masked generative image transformer," in *Proceedings of the IEEE/CVF Conference on Computer Vision and Pattern Recognition*, 2022, pp. 11315–11325.
- [24] Zhu Zhang, Jianxin Ma, Chang Zhou, Rui Men, Zhikang Li, Ming Ding, Jie Tang, Jingren Zhou, and Hongxia Yang, "M6-ufc: Unifying multi-modal controls for conditional image synthesis," *arXiv preprint arXiv:2105.14211*, 2021.
- [25] Shengju Qian, Huiwen Chang, Yuanzhen Li, Zizhao Zhang, Jiaya Jia, and Han Zhang, "Strait: Non-autoregressive generation with stratified image transformer," *arXiv preprint arXiv:2303.00750*, 2023.
- [26] Patrick Esser, Robin Rombach, and Bjorn Ommer, "Taming transformers for high-resolution image synthesis," in *Proceedings of the IEEE/CVF conference on computer vision and pattern recognition*, 2021, pp. 12873–12883.
- [27] William B Pennebaker and Joan L Mitchell, *JPEG: Still image data compression standard*, Springer Science & Business Media, 1992.
- [28] David S Taubman, Michael W Marcellin, and Majid Rabbani, "Jpeg2000: Image compression fundamentals, standards and practice," *Journal of Electronic Imaging*, vol. 11, no. 2, pp. 286–287, 2002.
- [29] Thomas Wiegand, Gary J Sullivan, Gisle Bjontegaard, and Ajay Luthra, "Overview of the h. 264/avc video coding standard," *IEEE Transactions on circuits and systems for video technology*, vol. 13, no. 7, pp. 560–576, 2003.
- [30] Wen Gao, Siwei Ma, Wen Gao, and Siwei Ma, "An overview of avc2 standard," *Advanced Video Coding Systems*, pp. 35–49, 2014.
- [31] Gary J Sullivan, Jens-Rainer Ohm, Woo-Jin Han, and Thomas Wiegand, "Overview of the high efficiency video coding (hevc) standard," *IEEE Transactions on circuits and systems for video technology*, vol. 22, no. 12, pp. 1649–1668, 2012.
- [32] Lucas Theis, Wenzhe Shi, Andrew Cunningham, and Ferenc Huszar, "Lossy image compression with compressive autoencoders," *arXiv preprint arXiv:1703.00395*, 2017.
- [33] Yoojin Choi, Mostafa El-Khamy, and Jungwon Lee, "Variable rate deep image compression with a conditional autoencoder," in *Proceedings of the IEEE/CVF International Conference on Computer Vision*, 2019, pp. 3146–3154.
- [34] Fei Yang, Luis Herranz, Joost Van De Weijer, José A Iglesias Guitián, Antonio M López, and Mikhail G Mozerov, "Variable rate deep image compression with modulated autoencoder," *IEEE Signal Processing Letters*, vol. 27, pp. 331–335, 2020.
- [35] Chenjian Gao, Tongda Xu, Dailan He, Yan Wang, and Hongwei Qin, "Flexible neural image compression via code editing," *Advances in Neural Information Processing Systems*, vol. 35, pp. 12184–12196, 2022.
- [36] Nick Johnston, Damien Vincent, David Minnen, Michele Covell, Saurabh Singh, Troy Chinen, Sung Jin Hwang, Joel Shor, and George Toderici, "Improved lossy image compression with priming and spatially adaptive bit rates for recurrent networks," in *Proceedings of the IEEE Conference on Computer Vision and Pattern Recognition*, 2018, pp. 4385–4393.
- [37] Mu Li, Wangmeng Zuo, Shuhang Gu, Debin Zhao, and David Zhang, "Learning convolutional networks for content-weighted image compression," in *Proceedings of the IEEE conference on computer vision and pattern recognition*, 2018, pp. 3214–3223.
- [38] Yueqi Xie, Ka Leong Cheng, and Qifeng Chen, "Enhanced invertible encoding for learned image compression," in *Proceedings of the 29th ACM international conference on multimedia*, 2021, pp. 162–170.
- [39] Renjie Zou, Chunfeng Song, and Zhaoxiang Zhang, "The devil is in the details: Window-based attention for image compression," in *Proceedings of the IEEE/CVF Conference on Computer Vision and Pattern Recognition*, 2022, pp. 17492–17501.
- [40] Johannes Ballé, David Minnen, Saurabh Singh, Sung Jin Hwang, and Nick Johnston, "Variational image compression with a scale hyperprior," *arXiv preprint arXiv:1802.01436*, 2018.
- [41] Jooyoung Lee, Seunghyun Cho, and Seung-Kwon Beack, "Context-adaptive entropy model for end-to-end optimized image compression," *arXiv preprint arXiv:1809.10452*, 2018.
- [42] Fabian Mentzer, Eirikur Agustsson, Michael Tschannen, Radu Timofte, and Luc Van Gool, "Conditional probability models for deep image compression," in *Proceedings of the IEEE Conference on Computer Vision and Pattern Recognition*, 2018, pp. 4394–4402.
- [43] Mu Li, Kede Ma, Jane You, David Zhang, and Wangmeng Zuo, "Efficient and effective context-based convolutional entropy modeling for image compression," *IEEE Transactions on Image Processing*, vol. 29, pp. 5900–5911, 2020.
- [44] David Minnen and Saurabh Singh, "Channel-wise autoregressive entropy models for learned image compression," in *2020 IEEE International Conference on Image Processing (ICIP)*, IEEE, 2020, pp. 3339–3343.
- [45] Ze Cui, Jing Wang, Shangyin Gao, Tiansheng Guo, Yihui Feng, and Bo Bai, "Asymmetric gained deep image compression with continuous rate adaptation," in *Proceedings of the IEEE/CVF Conference on Computer Vision and Pattern Recognition*, 2021, pp. 10532–10541.
- [46] Jun-Hyuk Kim, Byeongho Heo, and Jong-Seok Lee, "Joint global and local hierarchical priors for learned image compression," in *Proceedings of the IEEE/CVF Conference on Computer Vision and Pattern Recognition*, 2022, pp. 5992–6001.
- [47] Xiaosu Zhu, Jingkuan Song, Lianli Gao, Feng Zheng, and Heng Tao Shen, "Unified multivariate gaussian mixture for efficient neural image compression," in *Proceedings of the IEEE/CVF Conference on Computer Vision and Pattern Recognition*, 2022, pp. 17612–17621.
- [48] Aaron Van Den Oord, Oriol Vinyals, et al., "Neural discrete representation learning," *Advances in neural information processing systems*, vol. 30, 2017.
- [49] Justin Johnson, Alexandre Alahi, and Li Fei-Fei, "Perceptual losses for real-time style transfer and super-resolution," in *Computer Vision—ECCV 2016: 14th European Conference, Amsterdam, The Netherlands, October 11–14, 2016, Proceedings, Part II 14*, Springer, 2016, pp. 694–711.

- [50] Aaron Van den Oord, Nal Kalchbrenner, Lasse Espeholt, Oriol Vinyals, Alex Graves, et al., “Conditional image generation with pixelcnn decoders,” *Advances in neural information processing systems*, vol. 29, 2016.
- [51] Ashish Vaswani, Noam Shazeer, Niki Parmar, Jakob Uszkoreit, Llion Jones, Aidan N Gomez, Łukasz Kaiser, and Illia Polosukhin, “Attention is all you need,” *Advances in neural information processing systems*, vol. 30, 2017.
- [52] Doyup Lee, Chiheon Kim, Saehoon Kim, Minsu Cho, and Wook-Shin Han, “Autoregressive image generation using residual quantization,” in *Proceedings of the IEEE/CVF Conference on Computer Vision and Pattern Recognition*, 2022, pp. 11523–11532.
- [53] Chuanxia Zheng, Tung-Long Vuong, Jianfei Cai, and Dinh Phung, “Movq: Modulating quantized vectors for high-fidelity image generation,” *Advances in Neural Information Processing Systems*, vol. 35, pp. 23412–23425, 2022.
- [54] Songwei Ge, Thomas Hayes, Harry Yang, Xi Yin, Guan Pang, David Jacobs, Jia-Bin Huang, and Devi Parikh, “Long video generation with time-agnostic vqgan and time-sensitive transformer,” in *Computer Vision—ECCV 2022: 17th European Conference, Tel Aviv, Israel, October 23–27, 2022, Proceedings, Part XVII*. Springer, 2022, pp. 102–118.
- [55] Wilson Yan, Yunzhi Zhang, Pieter Abbeel, and Aravind Srinivas, “Videogpt: Video generation using vq-vae and transformers,” *arXiv preprint arXiv:2104.10157*, 2021.
- [56] Wenyi Hong, Ming Ding, Wendi Zheng, Xinghan Liu, and Jie Tang, “Cogvideo: Large-scale pretraining for text-to-video generation via transformers,” *arXiv preprint arXiv:2205.15868*, 2022.
- [57] Aditya Ramesh, Mikhail Pavlov, Gabriel Goh, Scott Gray, Chelsea Voss, Alec Radford, Mark Chen, and Ilya Sutskever, “Zero-shot text-to-image generation,” in *International Conference on Machine Learning*. PMLR, 2021, pp. 8821–8831.
- [58] Ming Ding, Zhuoyi Yang, Wenyi Hong, Wendi Zheng, Chang Zhou, Da Yin, Junyang Lin, Xu Zou, Zhou Shao, Hongxia Yang, et al., “Cogview: Mastering text-to-image generation via transformers,” *Advances in Neural Information Processing Systems*, vol. 34, pp. 19822–19835, 2021.
- [59] Yuchao Gu, Xintao Wang, Liangbin Xie, Chao Dong, Gen Li, Ying Shan, and Ming-Ming Cheng, “Vqfr: Blind face restoration with vector-quantized dictionary and parallel decoder,” in *Computer Vision—ECCV 2022: 17th European Conference, Tel Aviv, Israel, October 23–27, 2022, Proceedings, Part XVIII*. Springer, 2022, pp. 126–143.
- [60] Zhouxia Wang, Jiawei Zhang, Runjian Chen, Wenping Wang, and Ping Luo, “Restoreformer: High-quality blind face restoration from undergraded key-value pairs,” in *Proceedings of the IEEE/CVF Conference on Computer Vision and Pattern Recognition*, 2022, pp. 17512–17521.
- [61] P. Deutsch, “Deflate compressed data format specification version 1.3,” *RFC 1951, Internet Engineering Task Force*, 1996.
- [62] David Salomon, *Data Compression: The Complete Reference*, Springer Science & Business Media, 4th edition, 2004.
- [63] Toderici George, Theis Lucas, Johnston Nick, Agustsson Eirikur, Mentzer Fabian, Balle Johannes, Shi Wenzhe, and Timofte Radu, “Clic 2020: Challenge on learned image compression, 2020,” <https://www.tensorflow.org/datasets/catalog/clic>, 2020.
- [64] Nicola Asuni and Andrea Giachetti, “Testimages: a large-scale archive for testing visual devices and basic image processing algorithms. in proceedings of the conference on smart tools and applications in computer graphics,” 2014.
- [65] Phillip Isola, Jun-Yan Zhu, Tinghui Zhou, and Alexei A Efros, “Image-to-image translation with conditional adversarial networks,” in *Proceedings of the IEEE conference on computer vision and pattern recognition*, 2017, pp. 5967–5976.
- [66] Jia Deng, Wei Dong, Richard Socher, Li-Jia Li, Kai Li, and Li Fei-Fei, “Imagenet: A large-scale hierarchical image database,” in *2009 IEEE conference on computer vision and pattern recognition*. Ieee, 2009, pp. 248–255.
- [67] Richard Zhang, Phillip Isola, Alexei A Efros, Eli Shechtman, and Oliver Wang, “The unreasonable effectiveness of deep features as a perceptual metric,” in *Proceedings of the IEEE conference on computer vision and pattern recognition*, 2018, pp. 586–595.
- [68] Keyan Ding, Kede Ma, Shiqi Wang, and Eero P Simoncelli, “Image quality assessment: Unifying structure and texture similarity,” *IEEE transactions on pattern analysis and machine intelligence*, vol. 44, no. 5, pp. 2567–2581, 2020.
- [69] Mario Lucic, Karol Kurach, Marcin Michalski, Sylvain Gelly, and Olivier Bousquet, “Are gans created equal? a large-scale study,” *Advances in neural information processing systems*, vol. 31, 2018.
- [70] Gisle Bjontegaard, “Calculation of average psnr differences between rd-curves,” *ITU SG16 Doc. VCEG-M33*, 2001.
- [71] Dailan He, Ziming Yang, Weikun Peng, Rui Ma, Hongwei Qin, and Yan Wang, “Elic: Efficient learned image compression with unevenly grouped space-channel contextual adaptive coding,” *CVPR 2022*, 2022.
- [72] Jinming Liu, Heming Sun, and Jiro Katto, “Learned image compression with mixed transformer-cnn architectures,” *arXiv preprint arXiv:2303.14978*, 2023.
- [73] Liu Ziwei, Luo Ping, Wang Xiaogang, and Tang Xiaoou, “Dataset Name,” 2020.



Fig. 8. The qualitative comparison results of ELIC [71], LIC-TCM [72], and our method on the Kodak ataset [20]. The average bpp and LPIPS of each method is reported at bottom row.

APPENDIX

The supplementary material conducts an analysis of the complexity of both our proposed method and baseline model in terms of encoding and decoding time. (see Section A) Subsequently, qualitative results are presented in order to complement the findings outlined in the main paper. (see Section A) Finally, more restored images and their corresponding VQ-indices map visualizations with greater loss ratios are provided. (see Section A)

The computational complexity of classical methods VVC [2], BPG [1], and Cheng *et al.* [19], our models without fine-tuning training and our method is analyzed in terms of encoding and decoding time over the Kodak [20], Tecnick [64] and CLIC2020 [63] datasets as shown in Table III. Despite the difference in the coding devices and other factors, the comparative outcomes demonstrate the potential of the proposed approach for practical implementation.

TABLE III
ENCODING TIME AND DECODING TIME OF VVC [2], CHENG [19], BPG [1] AND MODELS WITHOUT FINE-TUNING TRAINING AND OUR PROPOSED METHOD AT THE KODAK [20], CLIC [63], TECNICK [64] DATASET.

Testing set	Method	Module	Time (ms)
Kodak [20]	VVC [2]	Encoder	26144.417
		Decoder	46.417
	BPG [1]	Encoder	242.750
		Decoder	198.920
	Cheng <i>et al.</i> [19]	Encoder	6403.136
		Decoder	12578.946
	Ours	Encoder	92.989
		Decoder	12.300
Tecnick [64]	VVC [2]	Encoder	36723.225
		Decoder	92.350
	BPG [1]	Encoder	367.530
		Decoder	393.470
	Cheng <i>et al.</i> [19]	Encoder	12319.671
		Decoder	27068.692
	Ours	Encoder	276.106
		Decoder	10.910
CLIC2020 [63]	VVC [2]	Encoder	48166.824
		Decoder	142.216
	BPG [1]	Encoder	613.110
		Decoder	478.470
	Cheng <i>et al.</i> [19]	Encoder	26071.742
		Decoder	58460.301
	Ours	Encoder	234.201
		Decoder	11.488

TABLE IV
OUR METHOD AND THE QUANTITATIVE RESULTS OF ELIC [71] AND LIC-TCM [72] ON THE KODAK [20] DATASET.

Method	BPP ↓	PSNR ↑	LPIPS ↓	FID ↓	DISTS ↓
ELIC [71]	0.0737	27.49	0.38	153.86	0.2
LIC-TCM [72]	0.1287	29.31	0.29	105.25	0.2
Ours	0.0695	21.86	0.17	54.60	0.1

We present more qualitative comparison results of BPG [1], VVC [2], Cheng *et al.* [19], ours w/o fine-tune and our method on the datasets of CLIC2020 [63] and Tecnick [64] in Fig. 9 and Fig. 10, Fig. 11, Fig. 12, respectively.

At the same time, we also conducted a qualitative and quantitative analysis of our method with several previously proposed generation-based image compression coding methods, ELIC [71] and LIC-TCM [72], as shown in Table IV and Fig. 8. Obviously, our method has better compression performance than the mentioned methods at low bit rates.

In addition, we conducted additional experiments on facial and text images rich in high-frequency information, as shown in Fig. 13 and Fig. 14. Obviously, our untrained method also has good reconstruction results on these images. If necessary, the reconstruction quality can be further improved through training on specific datasets.

Here we provide more restored images and visualizations of their VQ-indices map, with missing ratios α ranging from 0.1 to 0.4, as depicted in Fig. 15. Notably, as the missing ratio is over 0.2, a gradual decline in the restoration effect becomes apparent.



Fig. 9. The qualitative comparison results of BPG [1], VVC [2], Cheng *et al.* [19], ours w/o fine-tune and our method on the Tecnick dataset [64]. The bpp and LPIPS of each method are shown at the bottom of each image. In particular, ↓ indicates that lower is better.

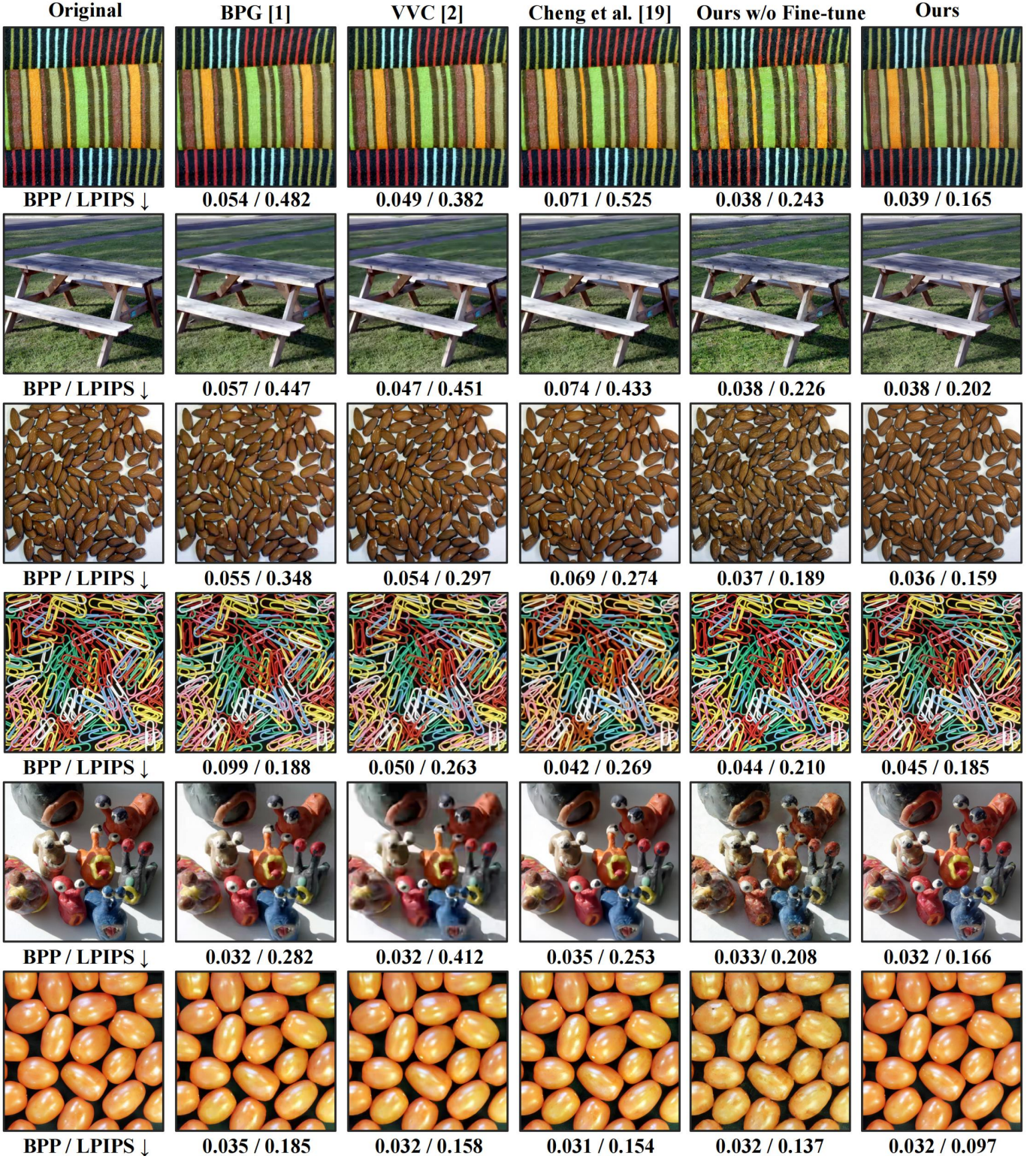


Fig. 10. The qualitative comparison results of BPG [1], VVC [2], Cheng *et al.* [19], ours w/o fine-tune and our method on the Tecnick dataset [64]. The bpp and LPIPS of each method are shown at the bottom of each image. In particular, ↓ indicates that lower is better.

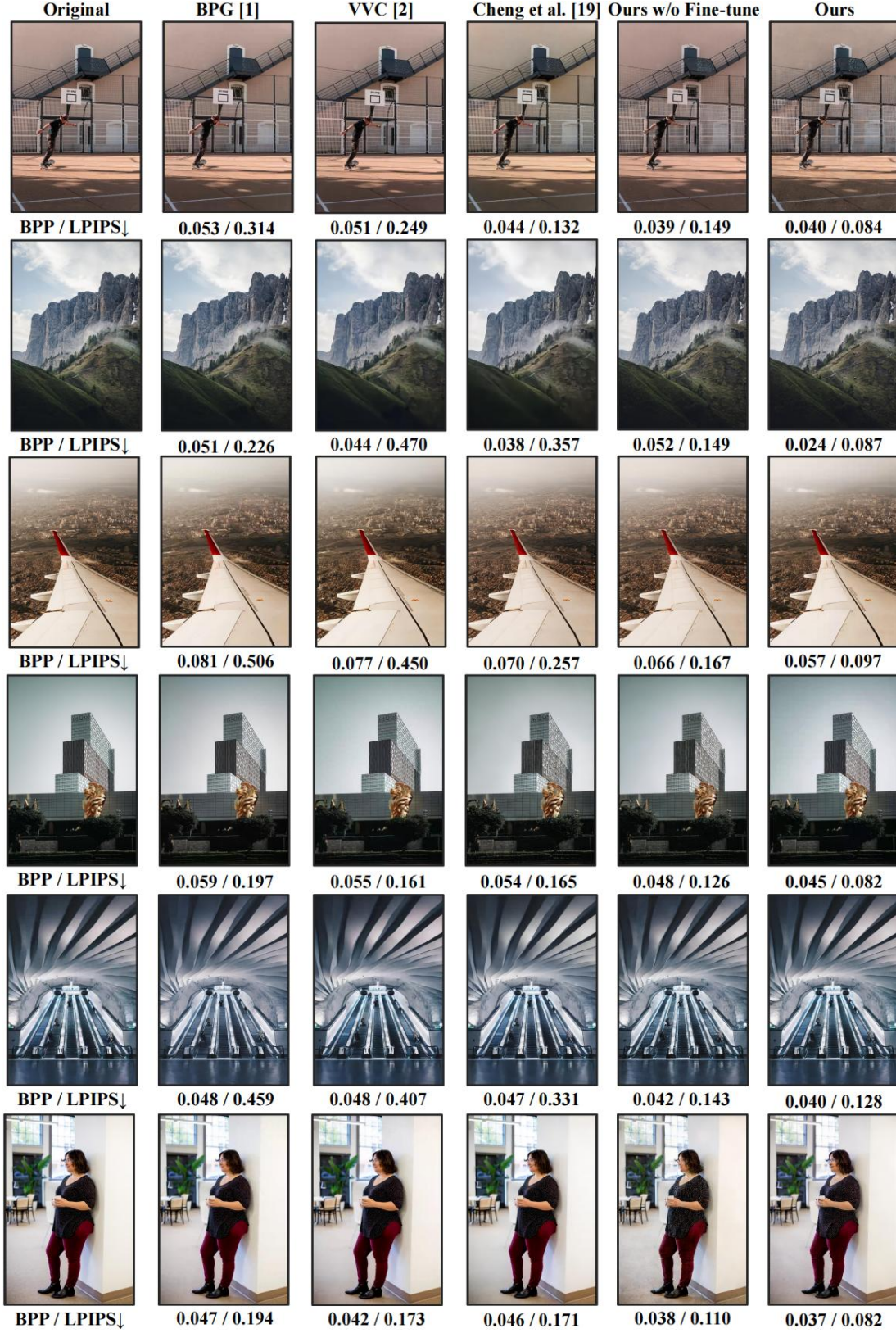


Fig. 11. The qualitative comparison results of BPG [1], VVC [2], Cheng *et al.* [19], ours w/o fine-tune and our method on the CLIC dataset [63]. The bpp and LPIPS of each method are shown at the bottom of each image. In particular, ↓ indicates that lower is better.

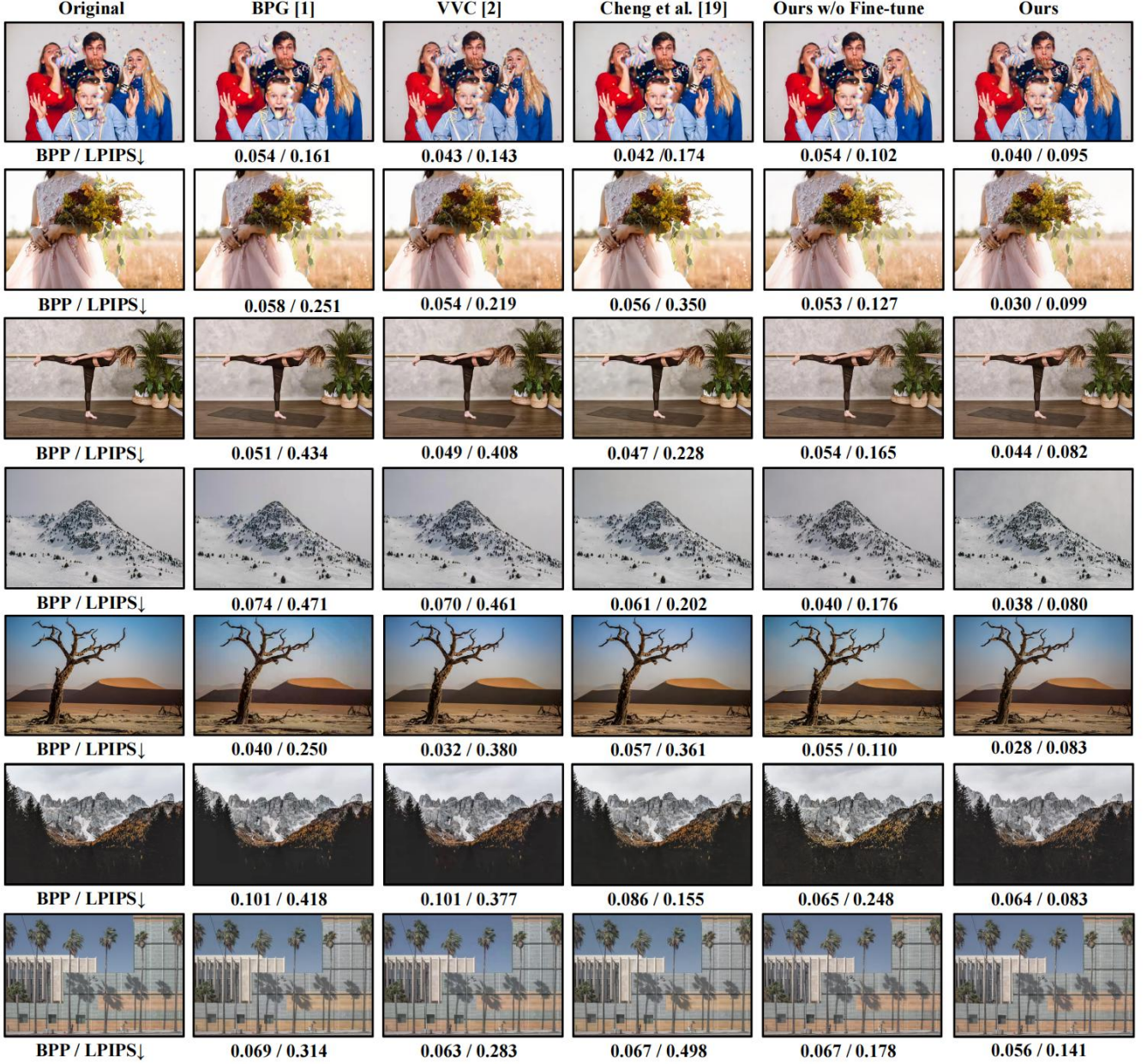


Fig. 12. The qualitative comparison results of BPG [1], VVC [2], Cheng *et al.* [19], ours w/o fine-tune and our method on the CLIC dataset [63]. The bpp and LPIPS of each method are shown at the bottom of each image. In particular, ↓ indicates that lower is better.

Original**BPP/LPIPS↓****Ours****0.062/0.16****BPP/LPIPS↓****0.060/0.07**

Fig. 13. Our method focuses on the additional results of facial images using the CelebA-HQ [73] dataset.



Fig. 14. Our method focuses on the additional results of text images using the CLIC2020 [63] dataset.

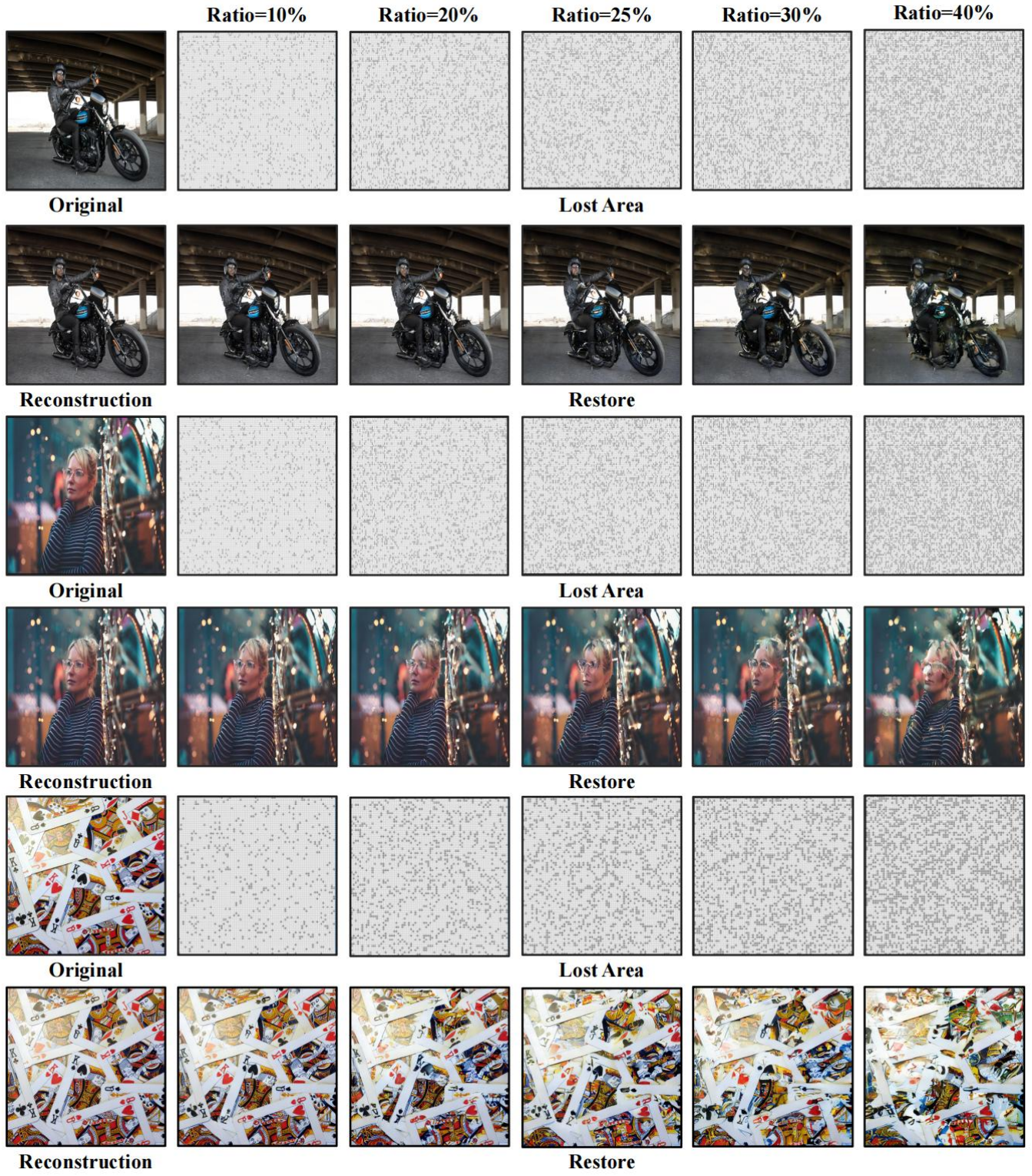


Fig. 15. Restored images with missing ratios ranging from 0.1 to 0.4. We also present a corresponding visual graph of the lost indices map, in which the black color corresponds to the indices that have been lost.